Different Methods for Direct Torque Control of Induction Motor Fed From Current Source Inverter

Aleksandar Nikolic *, Borislav Jeftenic **
* Department for electrical measurements, ** Electrical drives department.
* Electrical engineering institute "Nikola Tesla", ** University of Belgrade
* Koste Glavinica 8a, 11000 Belgrade, ** Bul. Kralja Aleksandra 73, 11000 Belgrade
Serbia
* anikolic@ieent.org http://www.ieent.org , ** jeftenic@etf.bg.ac.yu

Abstract: - Two different methods for direct torque control (DTC) of induction motor fed from current source inverter (CSI) is analyzed in the paper. The first one is derived from well-known DTC strategy developed for voltage inverter drives. This type of control basically uses hysteresis type controllers for torque and flux. In CSI drive there is only one controller used for torque control loop. The problems that arises in such a drive is significant torque pulsations due to the nature of CSI and occasional speed drops because of variable switching frequency. The other DTC method, proposed in the paper, is based on constant switching frequency with modification of the inverter optimal switching table. Further improvements are reduced number of sensors since all measurements are performed in DC link only and in flux estimator. Both simulation and experimental results shows that this algorithm has better performance without problems that exist in the same drive with torque hysteresis comparator. Finally, proposed method is simpler for implementation in a real drive without rotational transformation and parameter dependences that exist in vector control of the same drive.

Key-Words: - DTC, hysteresis comparator, constant switching, CSI, induction motor

1 Introduction

The direct torque control (DTC) is one of the actively researched control schemes of induction machines, which is based on the decoupled control of flux and torque. DTC provides a very quick and precise torque response without the complex field-orientation block and the inner current regulation loop [1], [2]. DTC is the latest AC motor control method [3], developed with the goal of combining the implementation of the V/f-based induction motor drives with the performance of those based on vector control. It is not intended to vary amplitude and frequency of voltage supply or to emulate a DC motor, but to exploit the flux and torque producing capabilities of an induction motor when fed by an inverter [4].

Although the traditional DTC is developed for voltage-source inverters, for synchronous motor drives the current-source inverter (CSI) is proposed [5], [6]. This type of converter can be also applied to DTC induction motor drive, and in the paper such an arrangement is presented. The induction motor drives with thyristor type current-source inverter (CSI, also known as auto sequentially commutated inverter) possess some advantages over voltage-source inverter drive. CSI permits easy power regeneration to the supply network under the breaking conditions, what is favorable in large-power induction motor drives. In traction applications bipolar thyristor structure is replaced with gate turn-off thyristor (GTO). Nowadays, current source inverters are popular in medium-voltage applications, where symmetric gate-commutated thyristor (SGCT) is utilized as a new switching device with advantages in PWM-CSI drives [7].

DTC of a CSI-fed induction motor involves the direct control of the rotor flux linkage and the electromagnetic torque by applying the optimum current switching vectors. Furthermore, it is possible to control directly the modulus of the rotor flux linkage space vector through the rectifier voltage [5]. Instead of triggering the rectifier voltage by the applied flux error [6], the current controller is used.

The reference current is formed from the components in synchronous frame – i_{sd}* obtained from the output of rotor flux PI controller and i_{sq}* calculated from the torque and rotor flux references. Similarly to the stator flux field-oriented control and DTC with constant switching frequency (space vector modulation – SVM [8]), current components i_{sd}* and i_{sq}* and reference rotor flux (Ψ_{rd}* = Ψ_r*, Ψ_{rq}* = 0) are used to calculate reference stator flux. Since flux estimator operates in stationary reference frame, it is necessary to convert input variables from

synchronous to stationary frame. This coordinate transformation is only performed when reference is changed and there is no influence to the dynamics of the control algorithm. To avoid some drawbacks of torque hysteresis controller (larger torque ripples, necessity to adopt torque hysteresis bandwidth depend on the motor speed), a phase angle between current components i_{sd}* and i_{sq}* is applied as a control variable. This angle is added to the rotor flux position and introduced to the flux sector seeker. As a result, the same current vector will be chosen as in the case of vector control algorithm [11], where coordinate transformation is employed to activate the inverter switches.

2 Main differences between two DTC methods

In a direct torque controlled induction motor drive supplied by current source inverter it is possible to control directly the modulus of the rotor flux-linkage space vector through the rectifier voltage, and the electromagnetic torque by the supply frequency of the CSI.

2.1 Hysteresis control DTC strategy

Basic DTC algorithm for CSI induction motor drive is derived using analogy from voltage source inverter (VSI) drive [5]. The inputs to the optimal switching table are the output of a 3-level hysteresis comparator and the position of the rotor flux-linkage space vector.

As a result, the optimal switching table determines the optimum current switching vector of current source inverter (Table 1).

Table 1: Optimum current switching-vector look-up table

ΔT_e	S_1	S_2	S_3	S_4	S_5	S_6
1	i_2	i_3	i_4	i_5	i_6	i_1
0	i_0	i_0	i_0	i_0	i_0	i_0
-1	i_6	i_1	i_2	i_3	i_4	i_5

According to the position of current space vector in CSI, if flux space vector is in sector S1, current vector i_2 should be selected for torque increase command. Similarly, for torque decrease command, i_6 should be selected (Fig. 1).

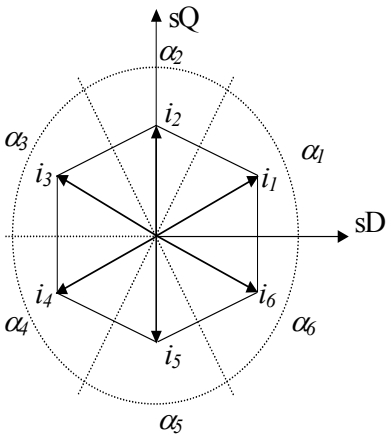

Fig. 1. Current space vector in CSI and its selection

Block diagram of this control strategy is shown in Fig. 2.

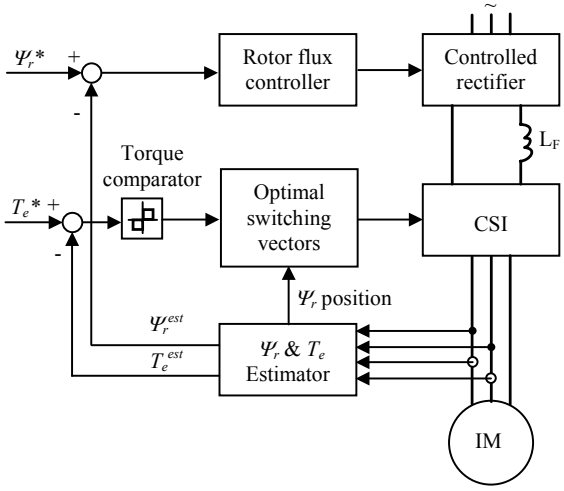

Fig. 2. DTC of CSI drive based on hysteresis control

It is necessary to emphasize the importance of zero space vectors. In VSI there are two zero voltage vectors: u_0 denotes case when all three switches from the one half of inverter are switched ON while u_7 represent state when switches are OFF. Contrary, in CSI (using analogy to the VSI) zero current vector i_0 represent case when all thyristors are OFF. That could lead to both torque and motor speed decrease. Due to the nature of commutation in CSI, it is convenient to keep the selected current vector at

instants when zero current vector is chosen. Torque response of the drive is shown in Fig. 3.

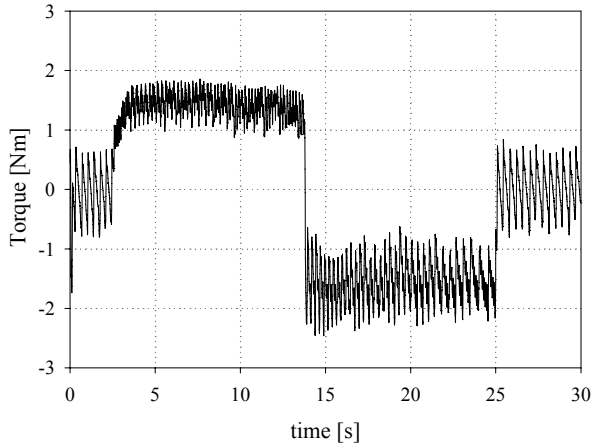

Fig. 3. Torque response in basic DTC drive

It could be observed that initial torque response is slower when the reference is lower, but it is fast during reversal since the torque reference change is doubled. On the other side, torque ripples are higher when torque changes its sign because torque-decreasing voltage vectors are stronger than the torque-increasing voltage vectors [8].

In that case, situation could be somewhat improved with modification of hysteresis comparator where positive part of hysteresis are larger then negative as shown in Fig. 4 [9].

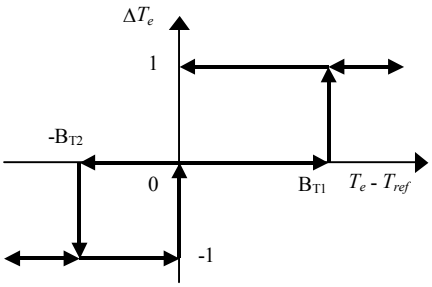

Fig. 4. Modified hysteresis comparator

2.2 Constant-switching DTC strategy

In DTC schemes, the presence of hysteresis controllers for flux and torque determines variable-switching-frequency operation for the inverter. Furthermore, using DTC schemes a fast torque response over a wide speed range can be achieved only using different switching tables at low and high speed. The problem of variable switching frequency can be overcome by different methods [5], [8]. In [8], a solution based on a stator flux vector control (SFVC) scheme has been proposed. This scheme may be considered as a development of the basic DTC scheme with the aim of improving the drive performance. The input commands are the torque and the rotor flux, whereas the control variables are the stator flux components. The principle of operation is based on driving the stator flux vector toward the corresponding reference vector defined by the input commands. This action is carried out by the space-vector modulation (SVM) technique, which applies a suitable voltage vector to the machine in order to compensate the stator flux vector error. In this way it is possible to operate the induction motor drive with a constant switching frequency.

In proposed DTC CSI drive shown in Fig. 5 the inputs are rotor flux and torque as in VSI presented in [8], but as a control variable the stator flux angle α_s is used.

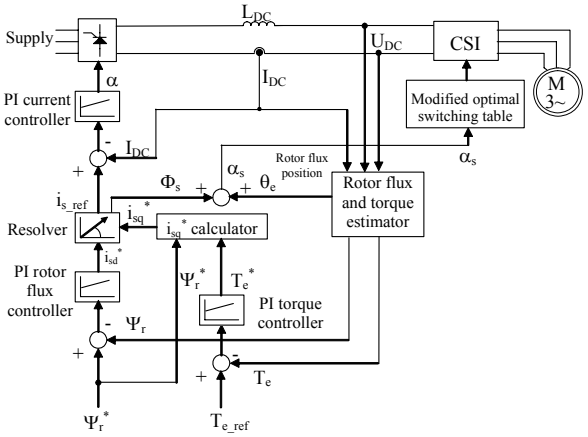

Fig. 5. Constant-switching DTC strategy in CSI fed induction motor drive

Although this configuration could remind on field-oriented control, the main difference is absence of coordinate transformation since it is not necessary to use coordinate transformation to achieve correct firing angle as in vector control of the same drive [11]. Identical result would be obtained when phase angle Φ_s between d-q current references and rotor flux vector angle $\theta_e = \arctan(\Psi_{r\beta}/\Psi_{r\alpha})$ are summed and resulting angle α_s is than used to determine sector of 60 degrees where resides rotor flux vector. In that way, phase angle Φ_s acts as a torque control command, since when reference torque is changed, i_{sq}^* is momentary changed.

Fig. 6 represent phasor diagram with reference current vector, rotor flux vector and corresponding angles.

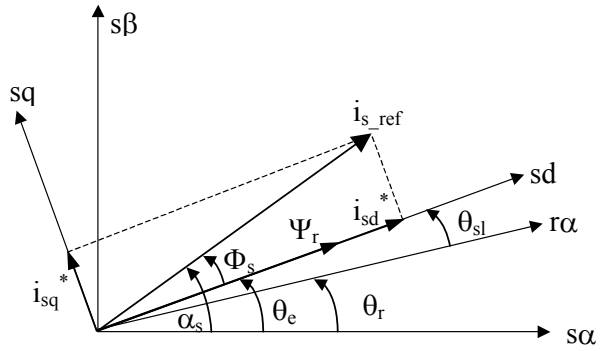

Fig. 6. Position of stator current and rotor flux vectors

Phase angle Φ_s "moves" stator current vector i_s in direction determined by the sign of torque reference and its value accelerate or decelerate flux vector movement according to the value of the reference torque (Fig. 7).

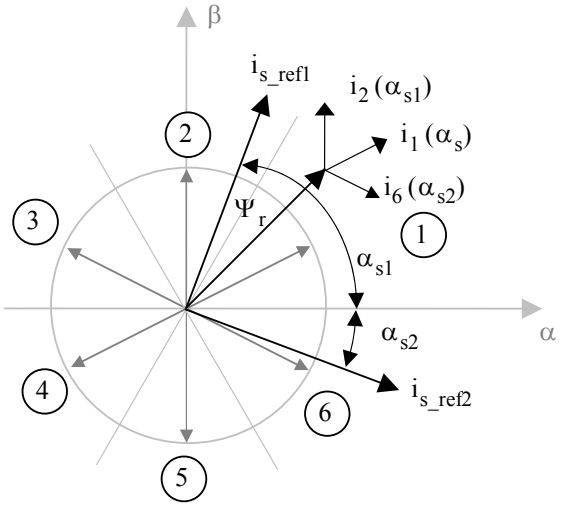

Fig. 7. Selecting proper current vector in proposed DTC algorithm

This modification implies somewhere different switching table for activating inverter switches, as shown in Table 2, where α_s is angle between referent α-axis and reference current vector i_s. That angle determines which current vector should be chosen: i_2 for torque increase, i_6 for torque decrease or i_1 for keeping torque at the current value.

Table 2: Optimal switching table in proposed DTC

Current vector	Angle range (degrees)
i_1	$\alpha_s > 0°$ and $\alpha_s \le 60°$
i_2	$\alpha_s > 60°$ and $\alpha_s \le 120°$
i_3	$\alpha_s > 120°$ and $\alpha_s \le 180°$
i_4	$\alpha_s > 180°$ or $\alpha_s \le -120°$
i_5	$\alpha_s > -120°$ and $\alpha_s \le -60°$
i_6	$\alpha_s > -60°$ and $\alpha_s \le 0°$

Torque response of the proposed method after the rated rotor flux is established is shown in Fig. 8. Comparing this result to that shown in Fig. 3 it could be observed that proposed method gives almost instant torque response with equal torque ripple width in both motor directions which means better speed repeatability when changing directions.

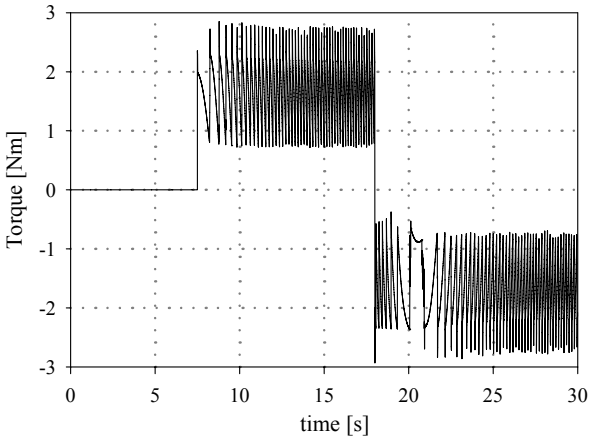

Fig. 8. Motor speed and torque response in open-loop speed control

3 Measuring and estimation

The stator flux value, needed for DTC control loop, is not convenient to measure directly. Instead of that, the motor flux estimation is performed [10], [12], [13]. In the voltage-based estimation method, the motor flux can be obtained by integrating its back electromotive force (EMF). The EMF is calculated from the motor voltage and current and the only motor parameter required is the stator winding resistance.

3.1 Input and control variables

The input variables of the proposed algorithm are motor torque T_e* and rotor flux amplitude Ψ_r*, as in the case of basic DTC. Control variables are current components in synchronous reference frame i_{sd}* and i_{sq}* and phase angle between them (Φ_s). D-axis component i_{sd}* is determined as the output of the PI rotor flux controller, while q-axis component i_{sq}* is calculated from the input variables and motor parameters:

$$i_{sq}^* = \frac{2 \cdot L_r}{3 \cdot p \cdot L_m \cdot \Psi_r^*} \cdot T_e^* \qquad (1)$$

where L_r is rotor inductance, L_m is mutual inductance and p denotes pair of poles.

Phase angle Φ_s and rectifier reference current are obtained as a result of rectangular to polar coordinate transformation:

$$\Phi_s = \arctan\left(\frac{i_{sq}^*}{i_{sd}^*}\right) \qquad (2)$$

$$i_{ref} = \sqrt{\left(i_{sd}^*\right)^2 + \left(i_{sq}^*\right)^2} \qquad (3)$$

The induction machine stator and rotor flux equations in terms of space vectors, written in a synchronous reference frame, are:

$$\overline{\Psi}_s = L_s \cdot \bar{i}_s + L_m \cdot \bar{i}_r \qquad (4)$$

$$\overline{\Psi}_r = L_r \cdot \bar{i}_r + L_m \cdot \bar{i}_s \qquad (5)$$

Substituting i_r in (4) and (5) the reference value of the stator flux vector in synchronous frame is determined, knowing the reference rotor flux and reference stator current:

$$\overline{\Psi}_s^* = \frac{L_m}{L_r} \cdot \overline{\Psi}_r^* + \frac{L_s \cdot L_r - L_m^2}{L_r} \cdot \bar{i}_s^* \qquad (6)$$

Since flux estimator operates in stationary reference frame, after coordinate transformation (6) become:

$$\Psi_{s\alpha\beta}^* = \frac{L_m}{L_r} \cdot \Psi_{r\alpha\beta}^* + \frac{L_s \cdot L_r - L_m^2}{L_r} \cdot i_{s\alpha\beta}^* \qquad (7)$$

where:

$$\begin{bmatrix} \Psi_{r\alpha}^* \\ \Psi_{r\beta}^* \end{bmatrix} = \begin{bmatrix} \cos\theta_e & -\sin\theta_e \\ \sin\theta_e & \cos\theta_e \end{bmatrix} \begin{bmatrix} \Psi_r^* \\ 0 \end{bmatrix} \qquad (8)$$

$$\begin{bmatrix} i_{s\alpha}^* \\ i_{s\beta}^* \end{bmatrix} = \begin{bmatrix} \cos\theta_e & -\sin\theta_e \\ \sin\theta_e & \cos\theta_e \end{bmatrix} \begin{bmatrix} i_{sd}^* \\ i_{sq}^* \end{bmatrix} \qquad (9)$$

and θ_e is rotor flux angle, i_{sd}* is output of rotor flux controller and i_{sq}* is given in (1).

3.2 Stator quantities identification

The voltage and the current of CSI fed induction motor, necessary for stator flux calculation, can be reconstructed from the DC link quantities knowing the states of the conducting inverter switches. In one duty cycle of the output current CSI has six commutations. In that case six intervals of 60 degrees can be defined in which the current and the voltage changes its values. In every interval the current from DC link flows through two inverter legs and two motor phase windings. The motor line voltage is equal to the DC voltage on the inverter input reduced for the voltage drop on the active semiconductors, i.e. serial connection of the thyristor and diode in each inverter leg. This voltage drop is forward voltage and for diodes it is about 0.7V-0.8V and for thyristors it is about 1V-1.5V. In this paper the average value of the overall forward voltage is used (2V), but for the practical realization it is chosen from the semiconductors datasheets or determined experimentally.

Fig. 9 presents the simplified equivalent circuit of the current source inverter used for the explanation of the proposed reconstruction method.

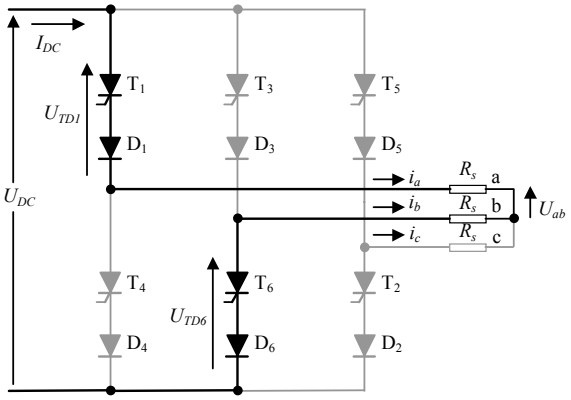

Fig. 9. Equivalent CSI circuit used for motor quantities detection

The currents in a,b,c phases in the first interval can be obtained directly from Fig. 9:

$$i_a = I_{DC},\ i_b = -I_{DC},\ i_c = 0, \qquad (10)$$

where I_{DC} is measured DC link current. The motor voltage U_{ab} is:

$$U_{ab} = U_{DC} - (U_{TD1} + U_{TD6}) \qquad (11)$$

where U_{TD1} and U_{TD6} is total voltage drops on the thyristor-diode par in leg 1 and 6, respectively. As mentioned before, the total voltage drop on the thyristor-diode par is V_F = 2V, and the motor voltage in this interval is now:

$$U_{ab} = U_{DC} - 2 \cdot V_F \qquad (12)$$

Using the previous analysis and Fig. 9 it can be generally concluded that the voltage drop on the corresponding thyristor-diode par could have the following values in dependence of the conducting thyristor T_x (x=1,…,6):

- $V_{TDx} = V_F$, when T_x is conducting,
- $V_{TDx} = 0.5 \cdot U_{DC}$ when conducts thyristor from the same half-bridge where T_x is,
- $V_{TDx} = U_{DC} - V_F$ when conducts thyristor from the same inverter leg where T_x is.

These results could be used for the voltage calculation in the other intervals, and they are summarized in Table 3.

Table 3: Motor current and voltage determined only by DC link measurements

	Active Thyristors	i_a	i_b	U_{ab}	U_{bc}
1	T1,T6	I_{DC}	0	$U_{DC} - 2 \cdot V_F$	$-0.5 \cdot U_{DC} + V_F$
2	T1,T2	I_{DC}	$-I_{DC}$	$0.5 \cdot U_{DC} - V_F$	$0.5 \cdot U_{DC} - V_F$
3	T3,T2	0	$-I_{DC}$	$-0.5 \cdot U_{DC} + V_F$	$U_{DC} - 2 \cdot V_F$
4	T3,T4	$-I_{DC}$	0	$-U_{DC} + 2 \cdot V_F$	$0.5 \cdot U_{DC} - V_F$
5	T5,T4	$-I_{DC}$	I_{DC}	$-0.5 \cdot U_{DC} + V_F$	$-0.5 \cdot U_{DC} + V_F$
6	T5,T6	0	I_{DC}	$0.5 \cdot U_{DC} - V_F$	$-U_{DC} + 2 \cdot V_F$

Prior to the flux estimation, the currents and voltages given in the Table 3 should be converted to the α-β stationary frame.

The resistance of the stator windings can be easily determined from the simple experiment when the motor is in the standstill. From Fig. 9 it can be seen that when only thyristors T_1 and T_6 conducts, the DC current will flow through motor phases *a* and *b*. Since the motor is in the standstill, the only voltage drop is on the stator resistance R_s:

$$U_{ab} = 2 \cdot R_s \cdot i_a \qquad (13)$$

when the windings are Y-connected. Generally, for the motor voltage value calculated in (12) and any type of the winding connection the stator resistance is:

$$R_s = \frac{U_{ab}}{k_s \cdot i_a} = \frac{U_{DC} - 2 \cdot V_F}{k_s \cdot I_{DC}} \qquad (14)$$

where k_s = 1 for Δ-connection and k_s =2 for Y-connection. Relation (14) can be easily implemented in the control software if the thyristors T_1 and T_6 are switched ON prior the motor start and the stator resistance is determined from the measured DC link current and voltage and the knowing voltage drop on the thyristor-diode par.

3.3 Flux and torque estimator

The main feedback signals in DTC algorithm are the estimated flux and torque. They are obtained as outputs of the estimator operating in stator reference frame. This estimator at first performs electro-motive force (EMF) integration to determine the stator flux vector:

$$\overline{\psi}_s^s = \int_0^t \left(\overline{u}_s^s - R_s \cdot \overline{i}_s^s \right) dt + \overline{\psi}_{s0}^s \qquad (15)$$

and than calculates the flux amplitude and find the sector of 60 degrees in α-β plane where flux vector resides, according to the partition shown in Fig. 7.

After the stator current and voltage are determined by reconstruction explained in the previous chapter, pure integrator in (15) yields flux vector, which components are subsequently limited in amplitude to the magnitude values of the stator flux references given by (7). The trajectory of flux vector is not circular in the presence of DC offset. Since its undisturbed radius equals Ψ_s^*, the offset components tend to drive the entire trajectory toward one of the $\pm\Psi_s^*$ boundaries.

A contribution to the EMF offset vector can be estimated from the displacement of the flux trajectory[9], as:

$$EMF_{\alpha\beta}^{off} = \frac{1}{\Delta t} \cdot \left(\Psi_{\alpha\beta\max} + \Psi_{\alpha\beta\min} \right) \qquad (16)$$

where the maximum and minimum values in (16) are those of the respective components $\Psi_{s\alpha}$ and $\Psi_{s\beta}$, and Δt is the time difference that defines a fundamental period. The signal EMF^{off} is fed back to the input of the integrator so as to cancel the offset component in EMF. The input of the integrator then tends toward zero in a quasi-steady state, which makes the estimated offset voltage vector equal the existing offset Ψ_{s0} in (15). The trajectory of Ψ_s is now exactly circular, which ensures a precise tracking of the EMF offset vector. Since offset drift is mainly a thermal effect that changes the DC offset very slowly, the response time of the offset estimator is not at all critical. It is important to note that the dynamics of stator flux estimation do not depend on the response of the offset estimator [9].

The estimated rotor flux is calculated from the stator flux estimate using motor parameters and reconstructed stator current:

$$\hat{\Psi}_{r\alpha\beta} = \frac{L_r}{L_m} \cdot \hat{\Psi}_{s\alpha\beta} - \frac{L_s \cdot L_r - L_m^2}{L_m} \cdot i_{s\alpha\beta} \qquad (12)$$

and its position in α-β reference frame is determined by:

$$\theta_e = \arctan\left(\frac{\Psi_{r\beta}}{\Psi_{r\alpha}}\right) \qquad (13)$$

Finally, from the estimated stator flux and reconstructed current vector the motor torque is:

$$T_e = \frac{3}{2} p \cdot \left(i_{s\beta}\Psi_{s\alpha} - i_{s\alpha}\Psi_{s\beta}\right), \qquad (14)$$

where the stator flux and current vectors are given in stationary α-β frame, and p denotes the number of poles.

4 Results

4.1 Modeling and simulation

The simulation model is developed in *Matlab/SIMULINK* [14], using *SimPowerSystems* block library that allows a very real representation of the power section (rectifier, DC link, inverter and induction motor). All electrical parameters (inductance of DC link, motor parameters) are the same as in real laboratory prototype with 4kW, 380V, 50Hz induction motor. Rated flux is 0.8Wb and rated torque is 14Nm. Rectifier reference current is limited to 12A and reference torque is limited to 150% of rated torque (20Nm).

The control algorithm is represented using *SIMULINK S*-function that gives possibility to write algorithms in C programming language as it will be in the real DSP controller.

Dynamical performances of DTC algorithm are analysed at first with rated flux and zero torque reference, than drive is accelerated up to 1000rpm. The speed is controlled in closed-loop via digital PI controller with following parameters:

- Proportional gain: $K_P = 5$,
- Integral gain: $K_I = 0.5$,
- Torque limit = 20Nm,
- Controller sampling time: $T_s = 4$ms.

The speed reference is set using succeeding scheme:

1) +1000rpm at t = 0.25s
2) –1000rpm at t = 0.6s.

As could be seen from Fig. 10 a fast torque response is achieved, with correct torque reference tracking and slow rotor flux ripple around the reference value (<1.5%).

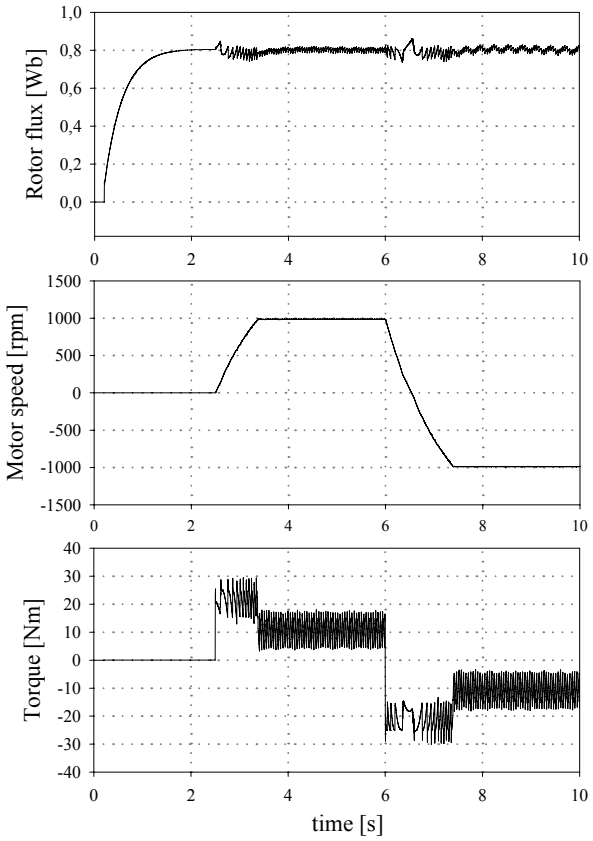

Fig. 10. Simulation results of proposed DTC method

4.2 Experiments

For experimental purposes a standard thyristor type frequency converter (three-phase bridge rectifier, DC link inductor and auto sequentially commutated inverter) is used. The CSI feeds a 4kW induction motor and, as a mechanical load, the DC machine with controlled armature current is used [11]. The algorithm presented in this paper is not dependent on the motor power or the type of switching devices and it could be applied to any current source converter topology. The low-power induction motor and standard type thyristors are used just for the simplicity of the laboratory tests.

The torque response is analyzed both with direct torque demand and under the closed-loop speed control. Speed controller is implemented with soft-start on its input and sample time of 20ms. Torque limit on the controller output is ±5Nm and is determined in such a way that under the maximum torque value slip is equal to maximal slip for current control:

$$s_{max} = \frac{1}{\omega_e \cdot T_r} = 0{,}0405 \qquad (15)$$

where ω_e is synchronous frequency (314rad/s) and T_r is rotor time constant (78.7ms).

Since rotor flux is not measured but determined by estimation, its value is checked with that obtained from simulation. Next figure shows this comparison between simulated and estimated rotor flux when zero speed reference and rated flux reference are given.

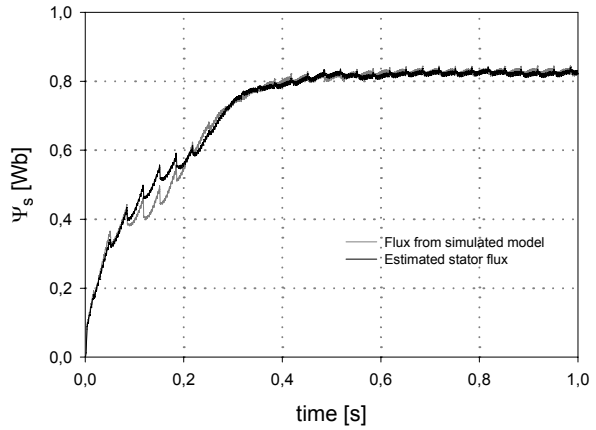

Fig. 11. Estimated and simulated rotor flux response

Good performance of the flux estimator, necessary for proper direct torque control, could be observed from Fig. 12, where flux trajectory is shown from the zero to its rated value. Almost circular flux trajectory with equal amplitudes in both α and β axes assures correct offset compensation.

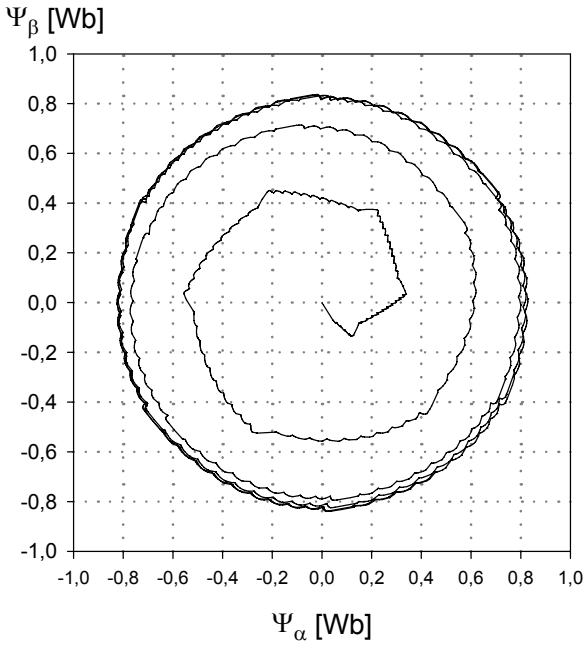

Fig. 12. Estimated rotor flux trajectory

Fig. 13 presents speed reversal when torque command is changed from 1.5Nm to –1.5Nm and vice versa.

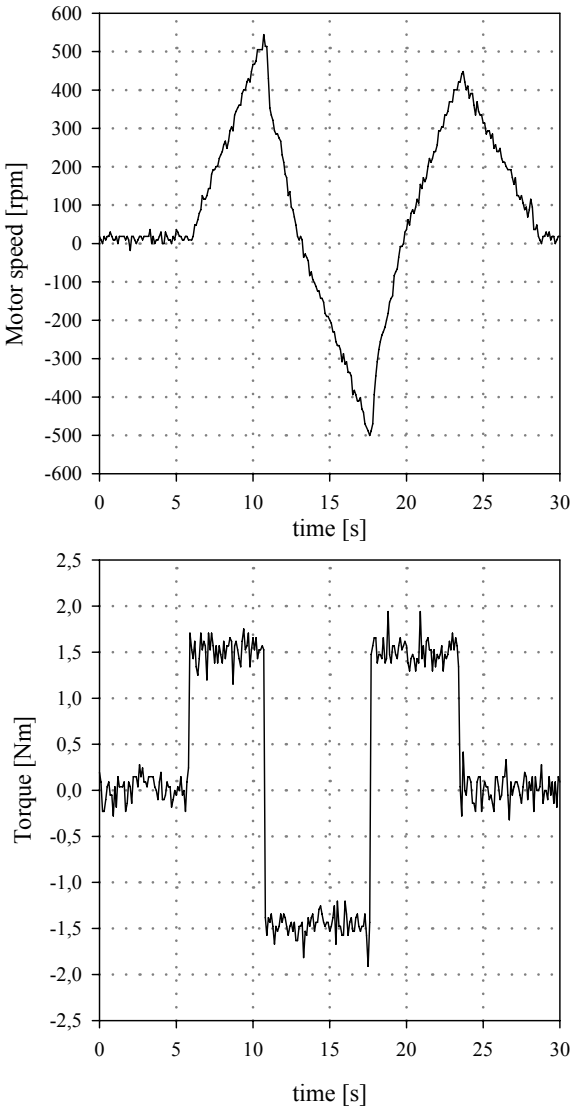

Fig. 13. Motor speed and torque response under square torque command

When the speed control loop is closed and reference speed is set to 500rpm from the standstill after the rated rotor flux is established, motor speed and torque response are recorded and shown in Fig. 14. Average torque value during accelerating period was 1.5Nm and in steady state when speed approaches 500rpm was about 0.3Nm.

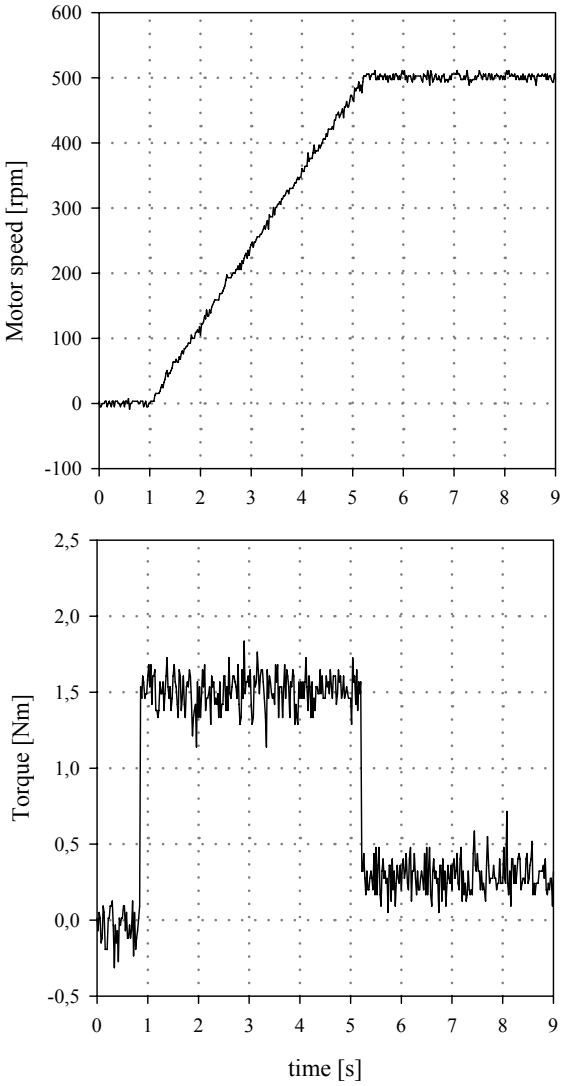

Fig. 14. Motor speed and torque response under closed-loop speed control

Motor speed and torque response during accelerating from 0rpm to 300rpm, than from 300rpm to 500rpm and back to 300rpm and 0rpm is shown in Figure 15.

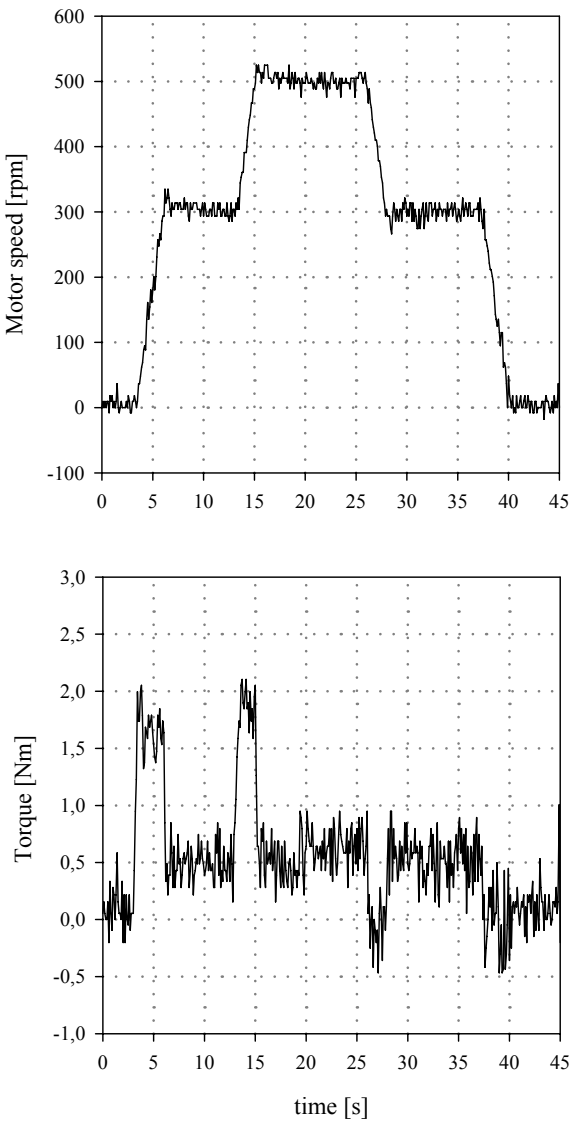

Fig. 15. Motor speed and torque response under different reference speed

Motor reversal from –500rpm to +500rpm in closed-loop speed control is shown in Fig. 16.

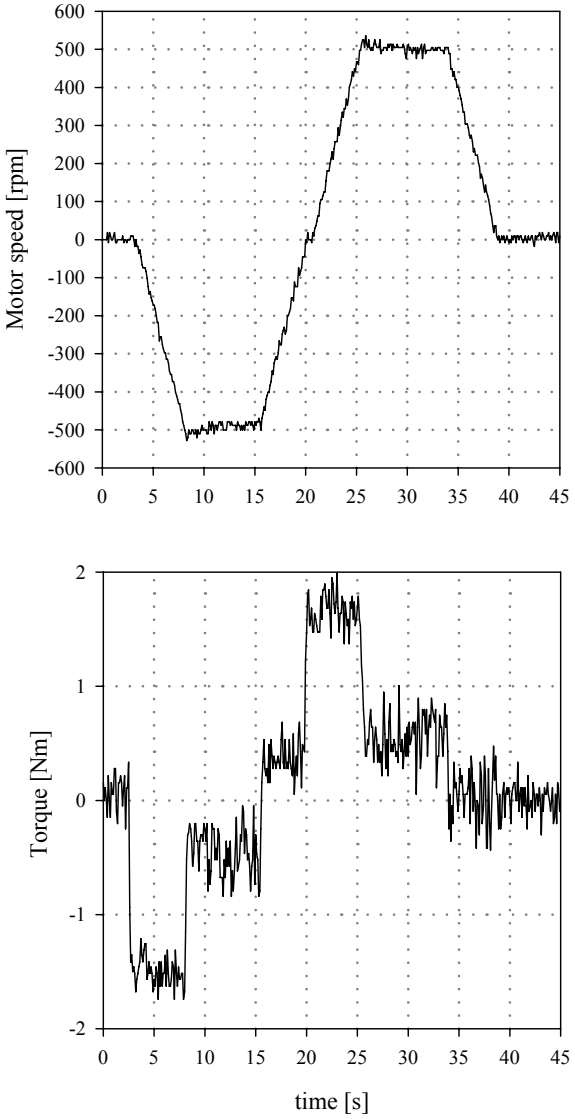

Fig. 16. Speed reversal during closed-loop control

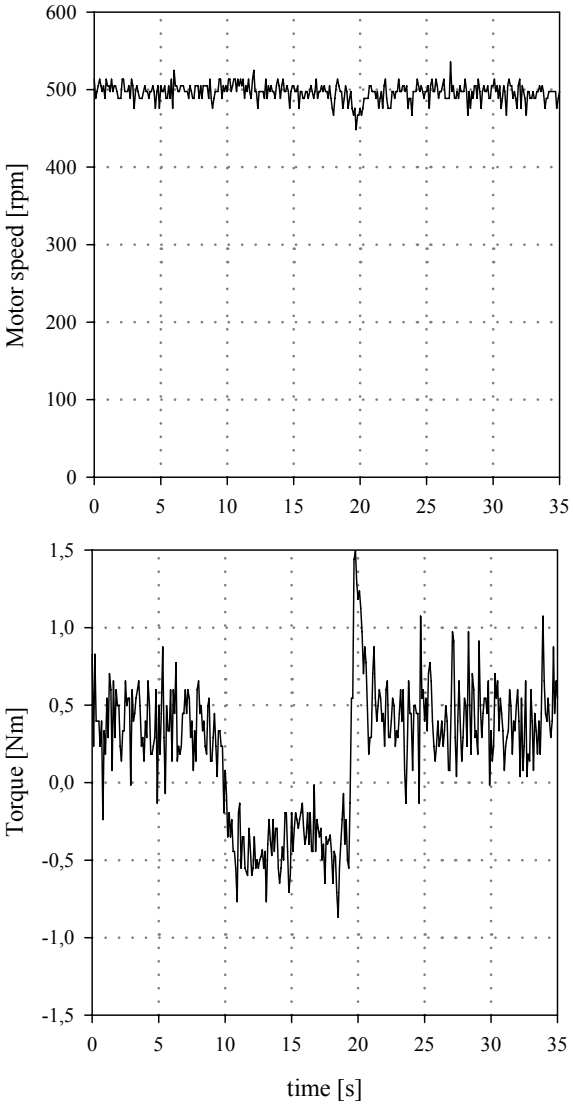

Fig. 17. Torque response during load changes

One of the merits of current source inverter, especially in high-power drives, is capability to regenerate power to the supply network under braking. Such experiment is done with current controlled 6kW DC machine used as a load (Fig. 17). After the rated rotor flux in induction motor is established, and the motor reaches steady state equal 500rpm, at t = 9s DC drive is switched ON. DC drive armature current is adjusted to the value that forces change of torque sign in induction machine. Than, CSI drive goes to braking regime to keep the speed at 500rpm. At t = 19s load is switched OFF and the sign of induction motor torque is positive again.

One of the important advantage of DTC is less sensitivity to parameter variations as could be expected in the vector controlled drive [11],[15],[16]. Contrary to the slip calculation using motor rotor time constant, proposed algorithm uses stator resistance for flux calculation and its value could be checked every time when motor is stopped using method explained in chapter 3.2. Other motor parameters (windings and mutual inductances) are used only when flux reference is changed and their values have no influence on the performance of the flux estimator due to the offset compensation.

4 Conclusion

Two different methods of direct torque control in CSI fed induction motor drive are presented in the paper. Contrary to the well-known hysteresis control derived from VSI drive, authors proposes new DTC algorithm based on the constant switching frequency.

Merit of such a solution in comparison to the vector control of the same drive is absence of coordinate transformation and speed sensor on the motor shaft. Furthermore, since flux estimator is based only on DC link measurements, there is not necessity for any sensor on the motor side which is one of main drive advantages.

In this case, by combination of vector control and basic DTC, a robust algorithm is developed that has a faster torque response and it is simpler for implementation. Moreover, algorithm is less sensitive to the parameter variation than standard FOC on the same drive. Only deterioration of drive performance could be expected under the speed of 100rpm due to the known problems of flux estimation. But, since CSI drive is not intended for low or zero-speed operation, this should not be treated as disadvantage.

Both results obtained by simulations and experiments on laboratory prototype have proved the validity of the proposed method.

References:

[1] I.Takahashi and T.Noguchi, A New Quick-Response and High-Efficiency Control Strategy of an Induction Motor, *IEEE Trans. on Industry Applications, Vol. 22*, 1986, pp. 820-827.

[2] M.Depenbrok, Direct Self-Control (DSC) of Inverter-Fed Induction Machine, *IEEE Trans. on Power Electronics, Vol.4*, 1988, pp. 420-429.

[3] P.Tiitinen, P.Pohjalainen and J.Lalu, The next generation motor control method: Direct Torque Control (DTC), *European Power Electronics Journal, Vol.5*, 1995, pp. 14-18.

[4] G.Buja, D.Casadei and G.Serra, Direct Stator Flux and Torque Control of an Induction Motor: Theoretical Analysis and Experimental Results, *The IEEE International Conference on Industrial Electronics IECON '98*, Bologna, Italy.

[5] P.Vas, *Sensorless Vector and Direct Torque Control*, Oxford University Press, U.K., 1998.

[6] I.Boldea, Direct Torque and Flux (DTFC) of A.C. Drives: A Review, *The 9th Conference EPE-PEMC 2000*, Kosice, Slovakia.

[7] N. R. Zargari, S. C. Rizzo, Y. Xiao, H. Iwamoto, K. Satoh, and J. F. Donlon, A new current-source converter using a symmetric gate-commutated thyristor (SGCT), *IEEE Transactions on Industry Applications, Vol.37*, 2001, pp. 896-903.

[8] D.Casadei, G.Serra, A.Tani, L.Zarri and F.Profumo, Performance Analysis of a Speed-Sensorless Induction Motor Drive Based on a Constant-Switching-Frequency DTC Scheme, *IEEE Transactions on Industrial Applications, Vol.39*, 2003, pp. 476-484.

[9] A.B.Nikolic, B.I.Jeftenic, Speed Sensorless Direct Torque Control Implementation in a Current Source Inverter Fed Induction Motor Drive, *The 35th IEEE Power Electronics Specialist Conference*, July 2004, Aachen, Germany.

[10] J.Holtz, Drift- and Parameter-Compensated Flux Estimator for Persistent Zero-Stator-Frequency Operation of Sensorless-Controlled Induction Motors, *IEEE Transactions on Industrial Applications*, *Vol.39*, 2003, pp. 1052-1060.

[11] A.Nikolic, B.Jeftenic, Precise Vector Control of CSI Fed Induction Motor Drive, *European Transactions on Electrical Power*, *Vol.16*, March 2006, pp. 175-188.

[12] A. Nesba, R. Ibtiouen, S. Mekhtoub, O. Touhami, S. Bacha, A New Approach to Main Flux Saturation Modeling of Induction Machine, *WSEAS TRANSACTIONS on CIRCUITS and SYSTEMS*, Issue 11, Volume 5, November 2006, pp. 1588-1596.

[13] G.Craciunas, Dynamic Flux Observer for Two-Phase Induction Motor Speed Control, *WSEAS TRANSACTIONS on CIRCUITS and SYSTEMS*, Issue 11, Volume 5, November 2006, pp. 1647-1654.

[14] E.Niculescu, E.P.Iancu, M.C.Niculescu, D.M.Purcaru, Analysis of PWM Converters using MATLAB, *WSEAS TRANSACTIONS on CIRCUITS and SYSTEMS*, Issue 10, Volume 5, October 2006, pp. 1522-1528.

[15] A.Onea, V.Horga, M.Ratoi, Indirect Vector Control of Induction Motor Based on Minimum Number of Parameters Model, *WSEAS TRANSACTIONS on CIRCUITS and SYSTEMS*, Issue 10, Volume 5, October 2006, pp. 1514-1522.

[16] Boukhelifa Akkila, Cheriti Ahmed, Ibtiouen Rachid, Touhami Omar, Current Minimization of a Field – Oriented Controlled Induction Machine Using Dynamic Programming Method and Parameters Sensitivity, *WSEAS TRANSACTIONS on CIRCUITS and SYSTEMS*, Issue 6, Volume 5, June 2006, pp. 837-843.